frontiers | Frontiers in Earth Science

TYPE Original Research
PUBLISHED 08 July 2025
DOI 10.3389/feart.2025.1580956

OPEN ACCESS

EDITED BY
Gordon Woo,
Risk Management Solutions, United Kingdom

REVIEWED BY
Chenliang Hou,
Anhui University of Science and Technology, China
Muhammad Shahab,
King Saud University, Saudi Arabia
Yunbo Li,
Henan Polytechnic University, China

*CORRESPONDENCE
Zhu Guanyu,
zhugy_cumt@163.com
Jiang Bo,
jiangbo@cumt.edu.cn

RECEIVED 21 February 2025
ACCEPTED 26 June 2025
PUBLISHED 08 July 2025

CITATION
Guanyu Z, Bo J, Ming L, Yu S and Guoxi C (2025) Logging identification of karstified Jurassic conglomerate aquifer in the Zhuxianzhuang coal mine: implications for water abundance heterogeneity and mining risk mitigation.
Front. Earth Sci. 13:1580956.
doi: 10.3389/feart.2025.1580956

Logging identification of karstified Jurassic conglomerate aquifer in the Zhuxianzhuang coal mine: implications for water abundance heterogeneity and mining risk mitigation

Zhu Guanyu[1,2]*, Jiang Bo[1,2]*, Li Ming[1,2], Song Yu[1,2] and Cheng Guoxi[1,2]

[1]Key Laboratory of Coalbed Methane Resource and Reservoir Formation Process, Ministry of Education, China University of Mining and Technology, Xuzhou, China, [2]School of Resources and Geosciences, China University of Mining and Technology, Xuzhou, China

The Jurassic conglomerate aquifer in the coal seam roof of Zhuxianzhuang Coal Mine in the Huaibei Coalfield exhibits significant karst and water-rich heterogeneity, and its geological patterns remain poorly understood. This study systematically investigates the lithology, stratigraphy, structural characteristics, karst features, and hydrogeological conditions of the Jurassic conglomerate aquifer. The conglomerate composition primarily consists of limestone, which undergoes intense and differential karstification and weathering. According to the fluctuation response characteristics of logging curves with different karst developments, a conglomerate aquifer karst logging identification model was constructed using apparent resistivity, artificial gamma, caliper, and acoustic time-difference as the key indicators. The aquifers were vertically classified into three types: intact section, relatively intact section, and broken section. Based on this classification and geological law, the vertical zonation and planar zonation characteristics were investigated. The conglomerate aquifers were further divided into four vertical development types: weathering crust type, karst type, composite type, and intact type, as well as six karst development planar zones. Influenced by the geological conditions of syncline structure, surface weathering and groundwater runoff, the overall distribution pattern of conglomerate aquifers demonstrates a progression from shallow to deep, transitioning from weathering crust types to composite, karst, and intact plane combinations.

KEYWORDS

Jurassic conglomerate aquifer, karst, logging identification, water abundance, geological control

1 Introduction

As one of the main factors affecting the safe production of coal, mine water hazards have received high attention (Hu and Tian, 2010; Zeng et al., 2024). Because of the complexity of water prevention and control work, many scholars have done a great deal of

research on the mechanism of coal mine water inrush and prevention theories from aspects such as stratigraphic lithology, geological structure, fracture development, topography and geomorphology. The lithology, thickness, water abundance, and solubility of aquifers determine the groundwater storage capacity and permeability (Guan et al., 2019; Li et al., 2022). Geological structures control the displacement and deformation of rock strata, influence the migration and accumulation of groundwater, and ultimately lead to the formation of water-rich areas (Song et al., 2013; Li et al., 2017). After coal seam mining, it will cause the movement and damage of overlying rock strata, leading to the expansion and connection of internal fractures in the rock strata and enhancing the conductivity of groundwater (Zhang and Zhang, 2020; Cao, 2020). The topography and geomorphology of the mining area determine the relationship between surface water and groundwater. Surface water can quickly recharge the underground aquifer through channels such as fractures and faults (Hou et al., 2020). Before coal seam mining, it is necessary to conduct hydrogeological surveys in the mining area to identify the water-conducting and water-bearing conditions of hidden disasters such as faults and collapse columns, as well as the water abundance of the rock strata in the roof and floor of the coal seam, so as to take targeted prevention and control measures.

Mainstream geophysical exploration technologies can accurately detect large-scale geological structures. However, the analysis of the structure of aquifer rock masses still requires the assistance of a large amount of geological drilling data. Therefore, it is of great practical significance and application value to accurately identify the rock stratum structure using drilling data. Geophysical logging uses acoustic, electrical, and radioactive equipment for detection. Rock strata with typical structures will give different responses in geophysical logging, enabling us to understand the changes in the physical and chemical properties of rock masses (Peng et al., 2008; Karacan, 2009; Fu et al., 2009; Hatherly, 2013; Lin et al., 2014). At present, research on the logging response characteristics of rock strata mainly focuses on lithology identification (Fang and Zhang, 2015; Gao and Li, 2016; Wu et al., 2016; Zhao et al., 2016; Wang, 2020), reservoir structure (Chen et al., 2013; Teng et al., 2015; Lai et al., 2017; Yin et al., 2019; Carrasquilla and Lima, 2020), and interpretation of carbonate karst strata (Liu et al., 2013; Guan et al., 2019; Tang and Zhao, 2019). In recent years, new technical means such as electrical imaging logging and nuclear magnetic resonance logging have also begun to be utilized in the identification of karst aquifer structures in carbonate rocks (Dlubac et al., 2013; Lopes et al., 2023; Ramadan et al., 2023). There is a lack of research on the structure of conglomerate aquifers in coal-bearing strata.

The hydrogeological conditions of Zhuxianzhuang coal mine in Huaibei are extremely complex. Mining the No. 8 coal seam (the main mining coal seam) is seriously threatened by the Jurassic conglomerate aquifer in the roof. This aquifer is a set of continental sediments with large lithological variations, large single-layer thickness, good water abundance, strong permeability, high water pressure, and strong heterogeneity (Zhu et al., 2018). During the mining of the 866 working face, a water and sand inrush accident occurred from the Jurassic conglomerate aquifer in the roof, resulting in significant economic losses. Therefore, Huaibei Mining Group promoted the comprehensive treatment project of curtain interception, dewatering, and mining of the Jurassic conglomerate aquifer in Zhuxianzhuang coal mine. However, due to the differences in the water abundance of the conglomerate aquifer, there is still a certain hydraulic head in some areas. Therefore, based on a systematic understanding of the geological characteristics, such as the lithological characteristics and thickness distribution of the conglomerate aquifer, it is urgent to research the development of karst and the distribution law of rock stratum structures.

This paper closely combines the observation of drill cores with the interpretation of logging curves, studies the logging response characteristics of different types of Jurassic conglomerate aquifer rock stratum structures, reveals the geological causes of the heterogeneity characteristics of the Jurassic conglomerate aquifer, determines the types of karst development in different planar zones in combination with the vertical differentiation of karst development, and evaluates the water abundance of each zone. The logging identification model and zoning method proposed in this study provide a scientific basis for mine water hazard prevention and control, and have important guiding significance and practical application value for the Huaibei coalfield, which is the first to conduct mining under the thick Jurassic piedmont proluvial conglomerate aquifer in the Huaibei coalfield.

2 Geological settings

The Suxian mining area is located in the southeastern of the Huaibei coalfield. In terms of the geotectonic environment, the Suxian mining area is situated at the southeastern margin of the North China plate, in the eastern part of the Yu-Huai depression and fold belt, and in the southern section of the Xuzhou-Suzhou arcuate duplex-imbricate fan thrust structure (Figure 1a) (Wang et al., 1998; Jiang et al., 2009). Zhuxianzhuang coal mine is located in the northeastern part of the Suxian mining area, in the northern section of the Sudong syncline in the overlying system of the southern section of the Xuzhou-Suzhou arcuate duplex-imbricate fan thrust structure (Figure 1b). The Sudong syncline is sandwiched between the Xisipo Fault and the Dongsanpu reverse fault (Li et al., 2023). It is an asymmetric syncline structure with an axial direction of NNW 330°–335°, a length of 18 km, and a width of approximately 1.5–5.8 km. The strata in the core of the syncline are from the Permian system.

The main mining coal seams in the area are the No. 8 coal seam in the Lower Shihezi formation system and the No. 10 coal seam in the Shanxi formation of the Permian. The Cenozoic loose layers overlie the Permian coal-bearing strata and are divided into four aquifers and three aquicludes from top to bottom. Among them, due to the characteristics of large thickness, stable distribution, and good water resistance of the third aquiclude, its existence makes the aquifers above the third aquifer and surface water have no water-filling impact on the ore deposit. The Quaternary sandstone aquifer (the fourth aquifer) directly overlies the sandstone fracture aquifer of the Permian coal measures, as well as the karst fracture aquifers of the Taiyuan formation and the Ordovician limestone. It not only creates hydraulic connections with the sandstone fractures of the coal measures but also serves as a passage

for groundwater communication among the bedrock aquifers, resulting in certain hydraulic connections among the bedrock aquifers. The Jurassic conglomerate aquifer is only developed in the northern part of the mining area. It has unconformable contacts with the underlying No. 8 coal seam and the overlying Cenozoic strata (Figure 2).

Due to the special contact relationships, there are obvious hydraulic connections between the Jurassic conglomerate aquifer and the other three major aquifers. Water in the Taiyuan limestone and Ordovician limestone can be directly replenished to the Jurassic conglomerate aquifer or indirectly replenished through the fourth aquifer, which constitutes the basic conditions for water inrush in the working face. Under the influence of mining disturbances, once the water-conducting fracture zone reaches the Jurassic conglomerate aquifer, in situations such as high water pressure, strong runoff, large static reserves, and strong dynamic recharge, it is highly likely to cause water inrush from the coal seam roof, threatening the safe mining of the working face.

3 Geological characteristics of the Jurassic conglomerate aquifer

The conglomerate rock strata in this study belong to the Sixian formation (J_3s) of the Upper Jurassic (Zhu et al., 2018). In the northern part of the study area, a large north Suzhou normal fault is developed, and the Sixian formation is locate in the upper wall of the fault. During the late Jurassic activity of the fault, Jurassic conglomerate was deposited in the diluvial facies of the foothills. The tectonic compression near EW direction of Yanshan Movement and the extension of Himalayan movement together caused the structural deformation of conglomerate aquifer and the formation of the NS syncline and F_{21} reverse fault structures.

3.1 Lithological characteristics

In this study, the systematic observation and identification of cores from 17 to 10, 17–12, 17–13, 18–3, 18–4, 19–5, 19–3 and surface 1 holes, combined with the analysis of data from 110 previous exploration holes, it can be inferred that the lithology of the Jurassic conglomerate aquifer primarily consists of gray-yellow, gray-red, and purplish-red conglomerate. It can be further divided into fine conglomerate, medium conglomerate and coarse conglomerate (Figure 3a). The gravel diameters vary, and the sorting is poor. The gravel composition is mainly limestone debris, followed by sandstone and metamorphic rock debris. The interstitial materials are mainly mud, coarse sand, and fine gravel, with basal cementation and calcareous-argillaceous cementation. After diagenesis, the conglomerate has suffered strong karstification and weathering, resulting in extremely strong heterogeneity. Karst development can be observed in some segments, with karst structures such as karst caves, karst fissures, and honeycomb-like karst erosion (Figure 3b).

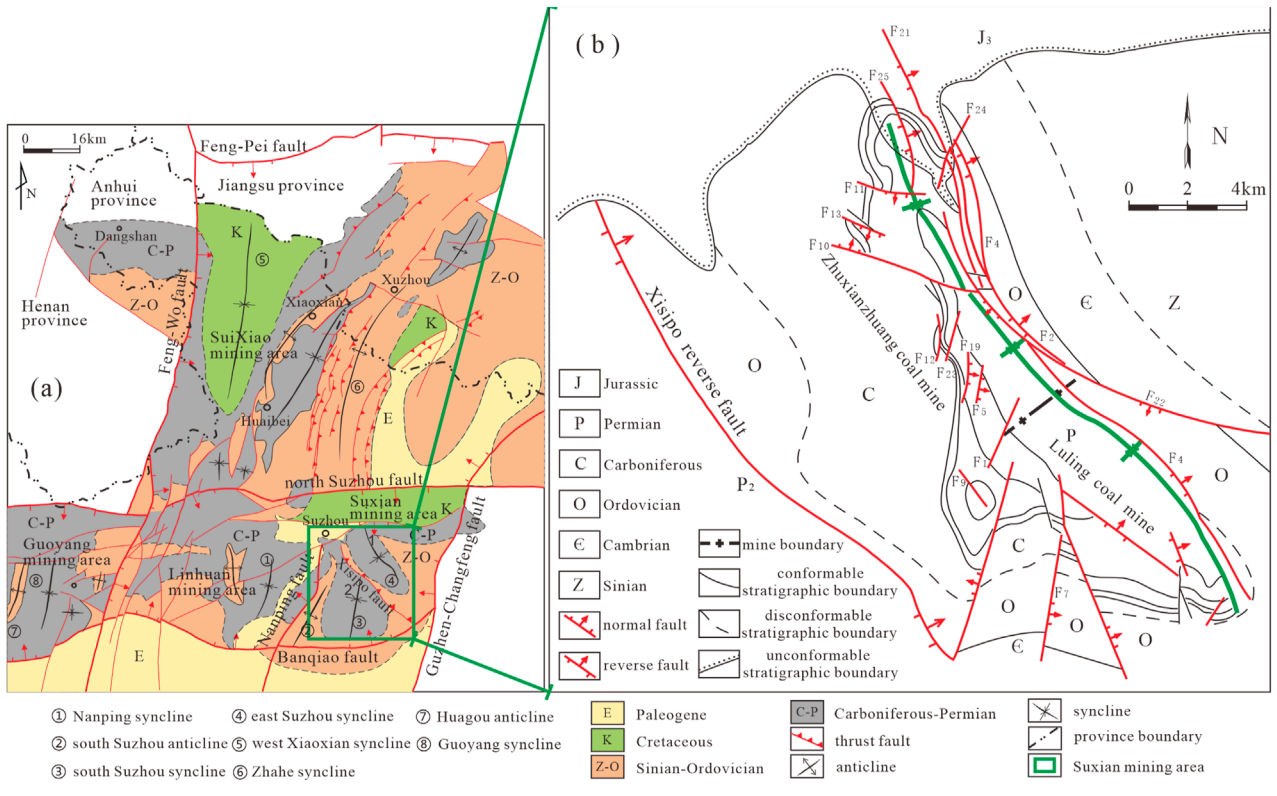

FIGURE 1
Structural outline map of the study area. (Modified from Jiang et al., 2010). **(a)** Huaibei coalfield, **(b)** Sudong syncline.

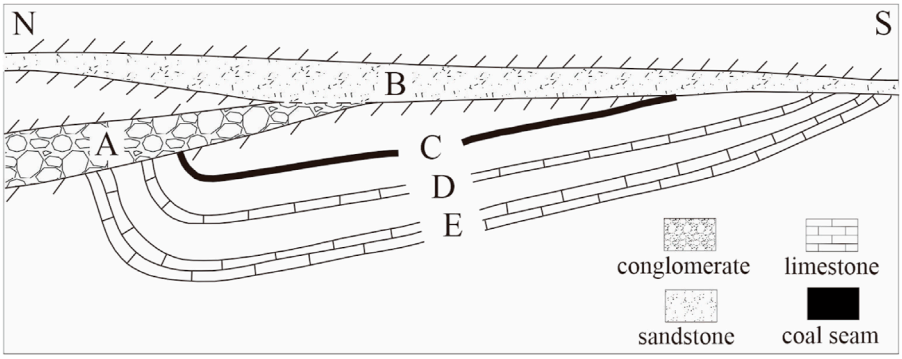

FIGURE 2
Major aquifers and contact relationships. **(A)** Jurassic conglomerate aquifer, **(B)** Sandstone aquifer (the fourth aquifer), **(C)** No. 8 coal seam, **(D)** Taiyuan limestone, **(E)** Ordovician limestone.

FIGURE 3
Lithological characteristics of the Jurassic conglomerate aquifer. **(a)** Overall view of core samples, **(b)** Local enlarged view of core samples.

FIGURE 4
Lithological characteristics of the Jurassic system. **(a)** Sand-mudstone segment, **(b)** Sand-gravel interbeds segment, **(c)** Conglomerate segment.

3.2 Strata characteristics

3.2.1 Vertical distribution characteristics

The analysis results of drill cores show that the Jurassic system in Zhuxianzhuang coal mine can be vertically divided into multi-layer structures: the upper sand-mudstone segment (Figure 4a), the middle sand-gravel interbeds segment (Figure 4b), and the lower conglomerate segment (Figure 4c). Controlled by the original stratigraphic deposition and subsequent tectonic denudation, the Jurassic system shows the development characteristics of stratigraphic combinations of single-layer, double-layer, and multi-layer structures (Figure 5). The strata with fully developed multi-layer structures are located at the alternating change positions of the sedimentary environment. The double-layer structure is

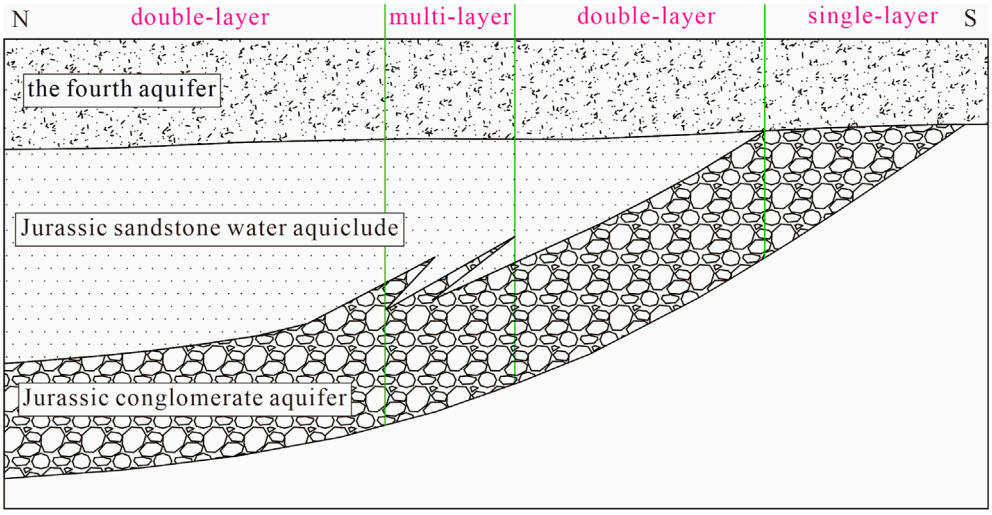

FIGURE 5
Strata association characteristics of the Jurassic system.

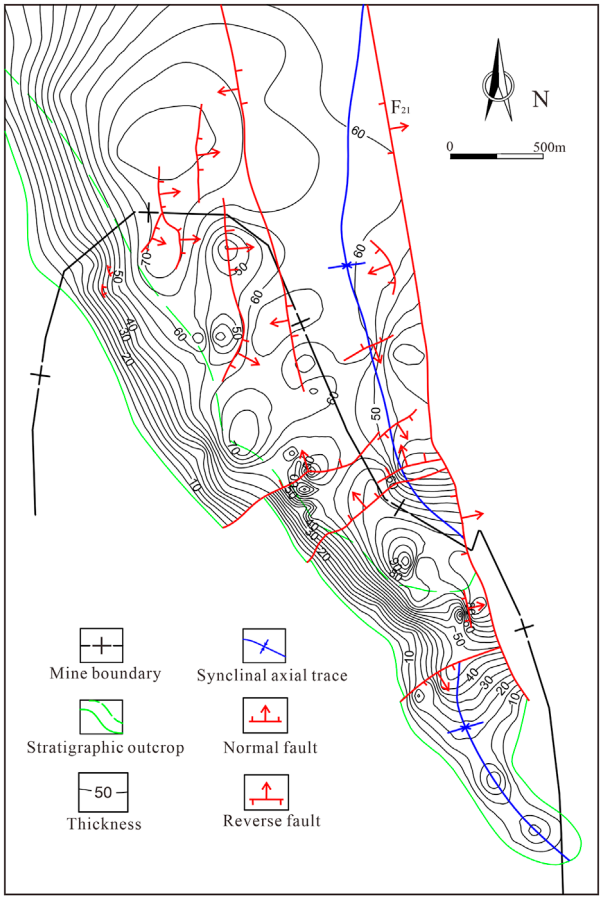

FIGURE 6
Thickness contours of the Jurassic conglomerate aquifer.

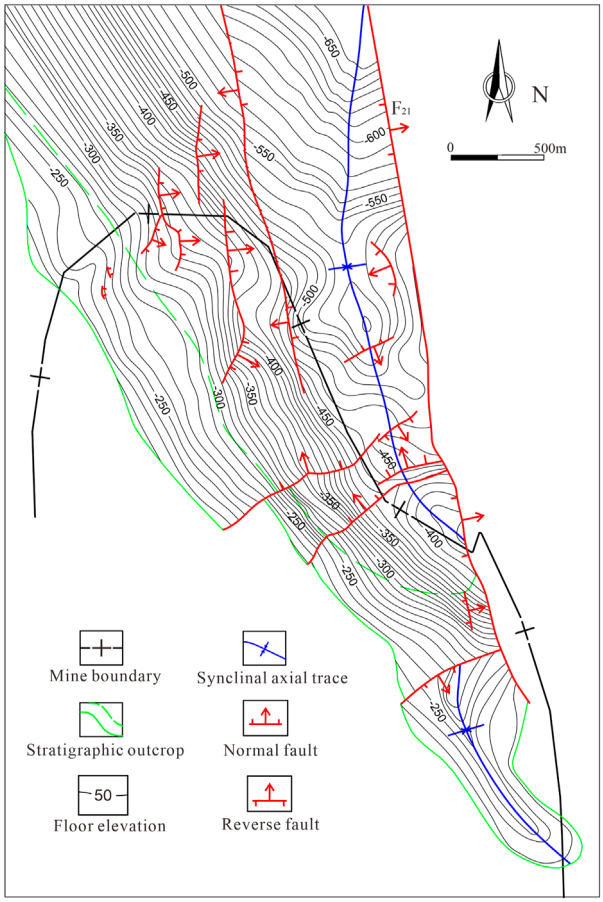

FIGURE 7
Floor elevation contours of the Jurassic conglomerate aquifer.

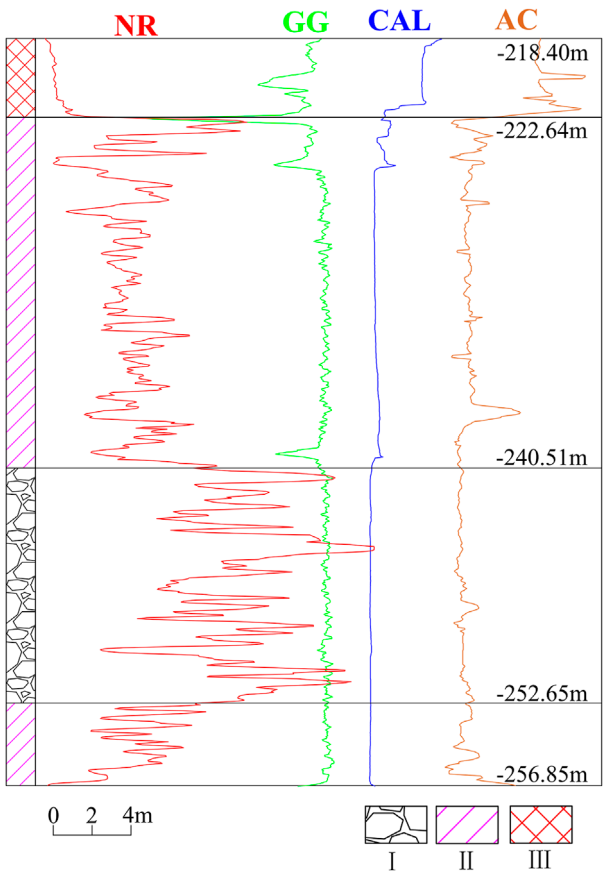

FIGURE 8
Logging identification model of rock mass structures.

generally a combination of the upper sandstone-shale segment and the lower conglomerate segment. And locally, it is a combination of the upper sand-gravel interbedded segment and the lower conglomerate segment, which is the product of the weathering and denudation of the top layer of the multi-layer structure. The single-layer structure is characterized by the development of only the conglomerate segment, which is the result of the weathering and denudation of the multi-layer or two-layer structure, leaving only the lower conglomerate segment. It can be seen that the conglomerate segment is stably developed at the bottom of the Jurassic system in the study area.

3.2.2 Planar distribution characteristics

The Jurassic conglomerate aquifer is distributed in the northeastern part of Zhuxianzhuang coal mine, covering an area of 2.8 km^2 in the mine field. It dips at an angle of 15°–25° and extends in a long tongue shape from north to south (Figure 6). The eastern side is truncated by the F_{21} reverse fault. The hanging wall of the fault has been denuded, and the Jurassic conglomerate aquifer in the footwall is in contact with the coal-bearing strata in the hanging wall, forming a water-resistant boundary. The western side is a concealed outcrop that unconformably contacts the bottom interface of the Cenozoic, that is, the direct contact zone between the fourth aquifer and the Jurassic conglomerate aquifer (Figure 2).

The distribution of the Jurassic conglomerate aquifer in the mine field is mainly affected by the morphology of the ancient bedrock surface and late denudation. Its thickness ranges from 0 to 110 m, averaging 50–65 m (Figure 6). The thickness distribution shows the characteristics of "thicker in the north and thinner in the south, thicker in the east and thinner in the west". At the same time, the Jurassic conglomerate aquifer with a thickness in the range of 0–50 m thickens rapidly along its stratigraphic dip direction, and the thickness is stable along the strike direction. It is manifested that the concealed outcrops in the west and south have been weathered and denuded, with relatively thin thicknesses, and they thicken rapidly towards the east and north, respectively. When the thickness is greater than 50 m, it is relatively stable, and the general thickness in the middle is 50–70 m.

The bottom boundary elevation of the Jurassic conglomerate aquifer ranges from −220 m to −660 m. The structural characteristics are controlled by the development of a near N–S-trending syncline that dips northward. The western wing is gentle and extends in the NW–SE direction; the eastern wing is relatively steep and is cut by the near NS - trending F_{21} reverse fault (Figure 7). The drop of the 13 faults developed in the area are all less than 40 m, and they cannot completely disconnect the Jurassic conglomerate aquifer.

4 Results and discussion

4.1 Logging response patterns of rock mass structures

The geophysical logging responses of damaged rock masses differ significantly from those of intact rock masses (Wu et al., 2016; Chen et al., 2013; Wang, 2015). Rock masses affected by karstification and weathering have more developed pores and fractures compared to intact rock masses. They also have stronger water-bearing and electrical conductivity capabilities. Under the action of an electric field, conductive ions can migrate more freely, resulting in a decrease in resistivity. The greater the decline in the apparent resistivity curve, the higher the degree of damage. Meanwhile, broken rock layers are more likely to experience diameter expansion during the drilling process, causing an increase in the caliper log value. The artificial gamma ray and acoustic time-difference curves also show an increase in amplitude due to the looser structure of the broken rock layers.

The study area has experienced multiple geological explorations in different periods, and many log curves lack quantitative digitization. In this study, it is found that there are broken and soft sections and karst-developed sections in the vertical direction of the Jurassic conglomerate aquifer, and its logging curve parameters have good response characteristics. Based on the above analysis, a rock mass structure identification model with four core indicators, namely apparent resistivity (NR), artificial gamma (GG), caliper (CAL), and acoustic time-difference (AC), was established. Combined with practical requirements, the rock mass structure of the Jurassic conglomerate aquifer was divided into three types: intact section (type I), relatively intact section (type II),

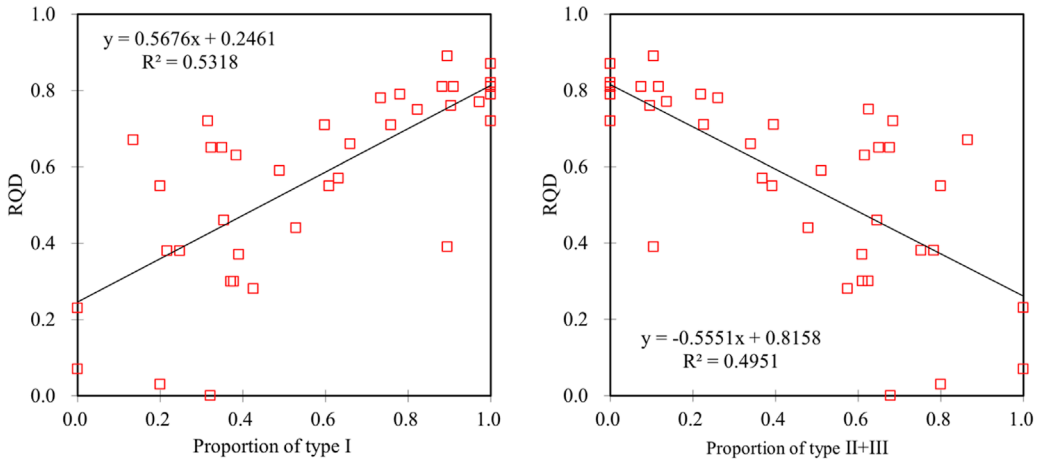

FIGURE 9
Relationship between rock mass structure proportions and rock quality designation. RQD-Rock quality designation, I- intact section, II- relatively intact section, III- broken section.

TABLE 1 Statistical table of karst rate.

Elevation (m)	Cumulative conglomerate thickness (m)	Cumulative cave length (m)	Average karst rate (%)
Over −300	801.85	70.76	8.82
−300~-350	168.91	22.16	13.12
−350~-400	121.76	1.01	0.83
Below −400	136.02	6.22	4.57

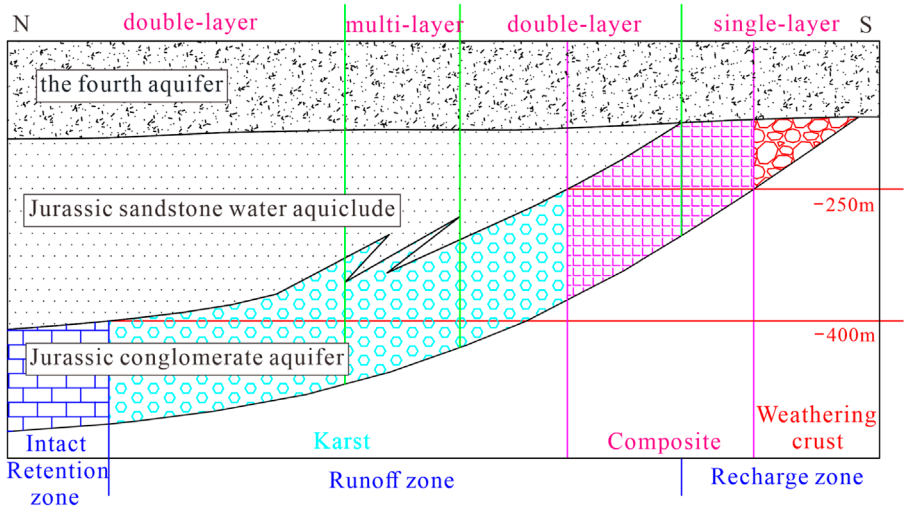

FIGURE 10
Vertical development types of Jurassic conglomerate aquifer.

and broken section (type III) (Figure 8). The intact section (type I) is characterized by its hardness and structural integrity, with no karst development. In contrast, the broken section (type III) shows notable karst development and rock mass fragmentation. The karst development in the relatively intact section (type II) lies between type I and type III, with smaller-scale karst features being present.

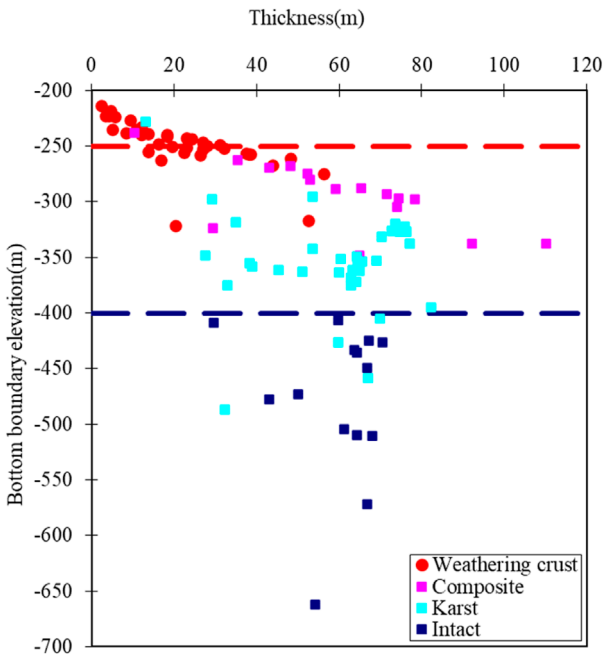

FIGURE 11
Comparison of vertical distribution and thickness of different developmental types.

NR-namely apparent resistivity, GG-artificial gamma, CAL-caliper, AC- acoustic time-difference, I- intact section, II- relatively intact section, III- broken section.

The logging interpretation results show that the NR and CAL curves respond well to the three types of rock mass structures. For type I structures, the NR is in the high-amplitude range and has finger-like fluctuations with large amplitudes; the CAL shows a low-amplitude value, and the curve is smooth and straight. For type II structures, the NR is in the medium-low amplitude range and can be distinguished from type III in most boreholes; the CAL value is generally slightly higher than that of type I and mostly shows wavy fluctuations. For type III structures, the NR is in the low-amplitude range; the CAL value is the highest, and due to different degrees of fragmentation, it often shows large amplitude finger-like fluctuations. These two curves can effectively distinguish between type I and type II structures.

The GG and AC curves are suitable for distinguishing type III structures. The reason is that the amplitudes of type I and type II structures on these two curves have a high overlapping range, while type III structures show obvious characteristics of low GG and high AC.

In summary, the logging curves of type I structures are characterized by "high NR, low CAL, high GG, and low AC", and the logging curves of type III structures are characterized by "low NR, high CAL, low GG, and high AC", and the amplitudes of the logging curves of type II structures are between those of type I and type III.

Based on the above identification model, the layered structure of the Jurassic conglomerate aquifer in the boreholes of the study area was divided, and the proportions of various rock mass structures were counted. Rock quality designation (RQD) is a quick, field-friendly metric for initial rock quality assessment. It quantifies the degree of fracturing in a rock mass by measuring the percentage of intact core pieces longer than 10 cm in a drill core sample (Barton et al., 1974). Through the comparative analysis of the proportions of different rock mass structures) (Figure 9), it can be seen that as the degree of karst development and fragmentation increases and the proportion of type II + type III increases, RQD and type I decrease linearly, reflecting the feasibility of the logging identification model. It also verifies the accuracy of the logging identification model.

4.2 Vertical structure types of the Jurassic conglomerate aquifer

The water-bearing capacity of the Jurassic conglomerate aquifer depends on the degree of karst development and the thickness of the Jurassic conglomerate aquifer, so there are differences in water-bearing capacity in different sections. According to the statistics of early exploration boreholes, the karst development rate is 8.82%–13.12% above - 350 m, and it decreases significantly below - 350 m, with a karst rate of only 0.83%–4.5% (Table 1). The characteristic that the degree of karst development in conglomerate decreases significantly with the increase of burial depth is also reflected in the statistics of the visible rate of karst in boreholes.

Based on the rock mass structure identification model, we interpret 129 boreholes in the study area. Combining the vertical distribution characteristics of the Jurassic conglomerate aquifer and the vertical differentiation of karst development, the Jurassic conglomerate aquifer was divided into 4 development types in the vertical direction (Figure 10).

4.2.1 Weathering crust type

Karst develops at the top or throughout the Jurassic conglomerate aquifer, which formed as a result of ancient weathering processes. The rock mass is broken and filled with yellow clay, with the characteristics of "thin thickness, shallow burial depth, low strength, weak water-bearing capacity, and low permeability". Borehole core observation and logging identification studies show that the paleo-erosion base level of the weathered-crust type generally develops at around - 250 m, with a thickness of less than 60 m (Figure 11). The formation reason is that the rock layers are cut by the unconformity interface of the Quaternary at the top and weathered and eroded, rather than formed by primary sedimentation (Figure 12). At the same time, its tectonic location also leads to a relatively shallow burial depth (Figure 13). The rock mass in this section is broken and difficult to core, with a low RQD value (Figure 14). The logging response shows a type III structure. The specific discharge (q) and permeability coefficient (K) obtained from the pumping test during hydrogeological exploration can reflect the water richness of the aquifer. However, due to the karst caves and fissures being filled with mud and sand, which effectively block the infiltration of water, the leakage in this layer during drilling period is relatively weak, and the hydrogeological parameters q and K are relatively low (Figures 3a,15).

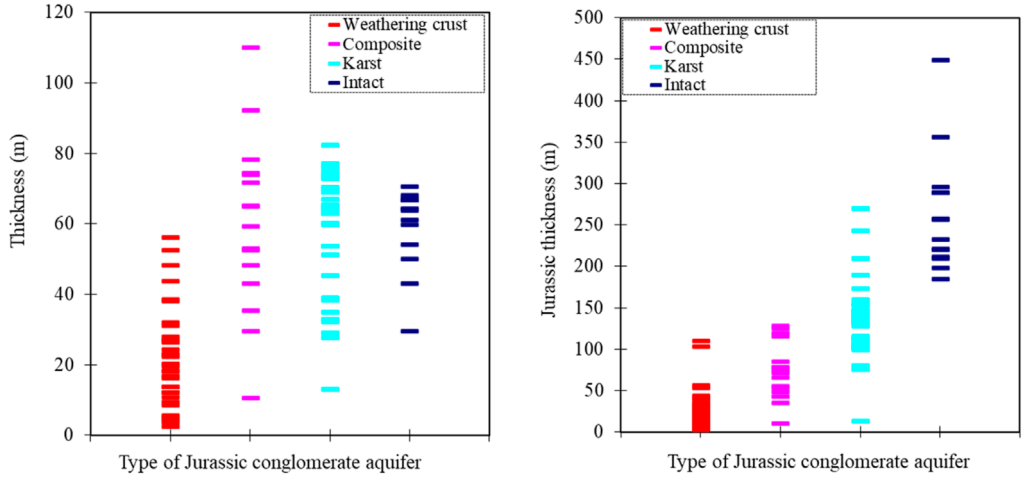

FIGURE 12
Thickness of different developmental types and corresponding Jurassic thickness.

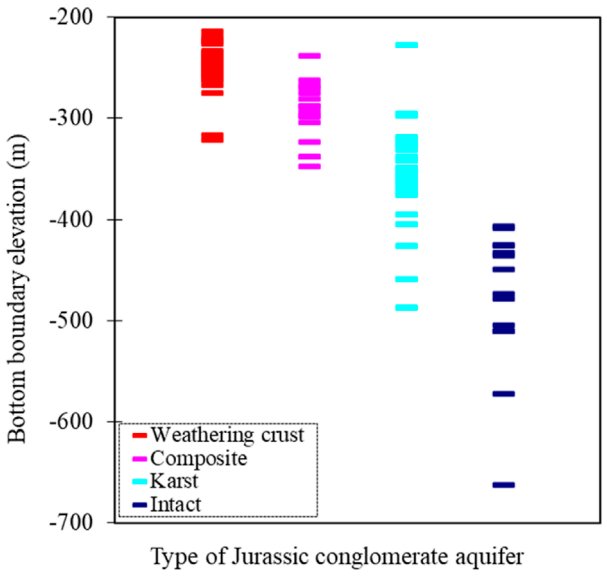

FIGURE 13
Comparison of floor elevation of different developmental types.

4.2.2 Karst type

Karst develops throughout or in multiple layers of the Jurassic conglomerate aquifer, with the characteristics of "large thickness, medium burial depth, low strength, strong water-bearing capacity, and high permeability". The thickness of the rock layer is 30–70 m, with large variations (Figure 12); the bottom boundary elevation is mostly between - 250 m and - 400 m (Figure 13). Karst types such as karst caves, karst fissures, and karst pores are highly developed, with strong heterogeneity and a significant reduction in rock quality (Figure 14); most karst pores are unfilled, and the measured hydrogeological parameters q and K are both high (Figure 15), belonging to a strong water-bearing area.

4.2.3 Composite type

There are multiple karst-developed layers in the Jurassic conglomerate aquifer, which is the product of the co-development of the upper weathered-crust type and the lower karst type. It shows different karst development characteristics at different elevation ranges. The part above - 250 m shows the characteristics of the weathered-crust type, while the part below −250 m shows the characteristics of the karst type (Figure 10). The RQD value of this type is between the weathering crust and the karst type (Figure 14), and the parts with intense water richness are mainly concentrated in the karst type. The measured hydrogeological parameters q and K are higher than that of the weathering crust type and slightly higher than that of the karst type (Figure 15), belonging to a strong water-bearing area.

4.2.4 Intact type

The rock mass is hard and intact, and karst does not develop. It has the characteristics of "large thickness, large burial depth, high strength, weak water-bearing capacity, and low permeability". The thickness of the rock layer is generally 60–70 m (Figure 12), and the bottom boundary elevation is mostly below - 400 m (Figure 13); the RQD of this type of rock mass can reach 70%–90%, the rock is hard and intact (Figure 14), the logging response shows a type I structure; the measured hydrogeological parameters q and K are both tiny (Figure 15), belonging to a weak water-bearing area.

4.3 Regional distribution characteristics of the Jurassic conglomerate aquifer structures

By integrating the vertical structure type division and plane distribution characteristics, the Jurassic conglomerate aquifer was divided into four types and six karst-developed areas (Figure 16).

(1) Recharge-weathering zone (A): It is located within the intersection range of the bottom and top boundaries of

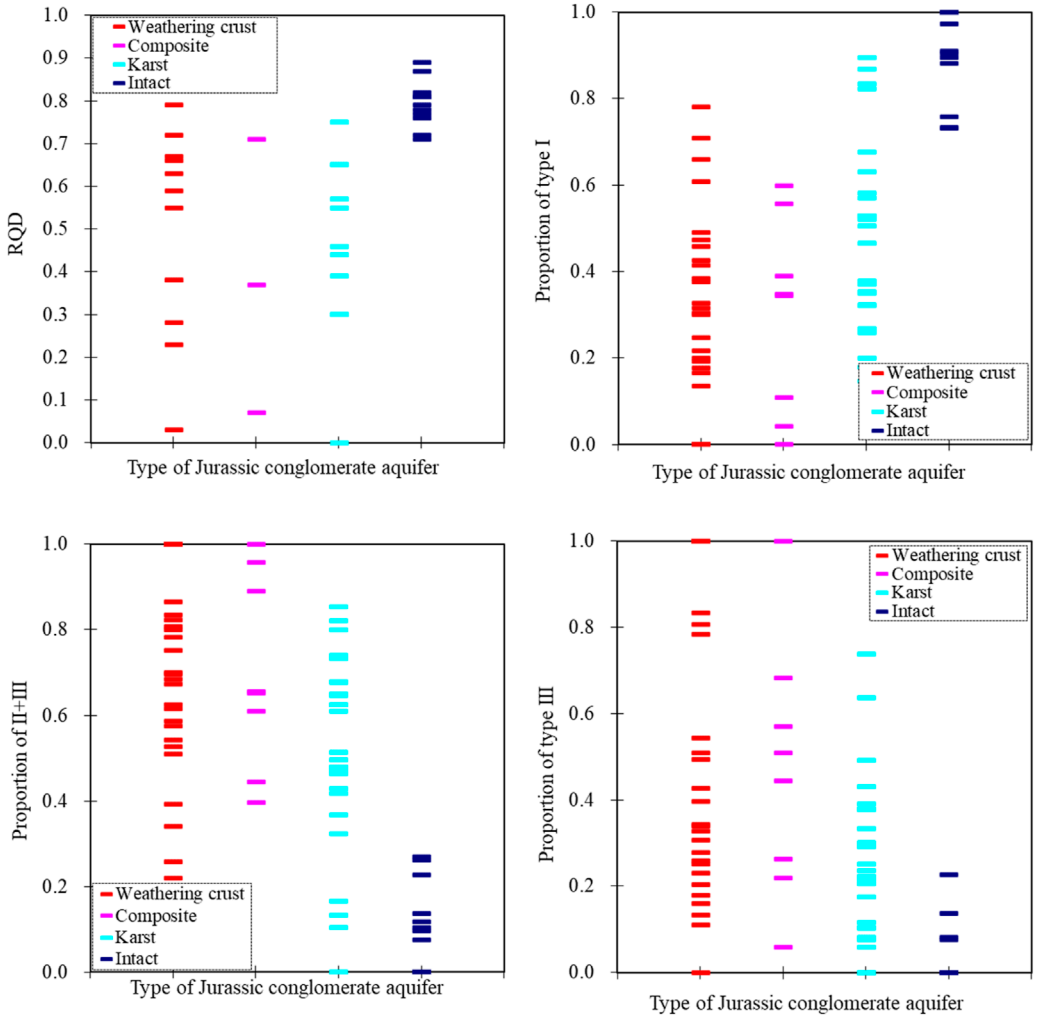

FIGURE 14
Comparison of RQD and stratified structure of different developmental types.

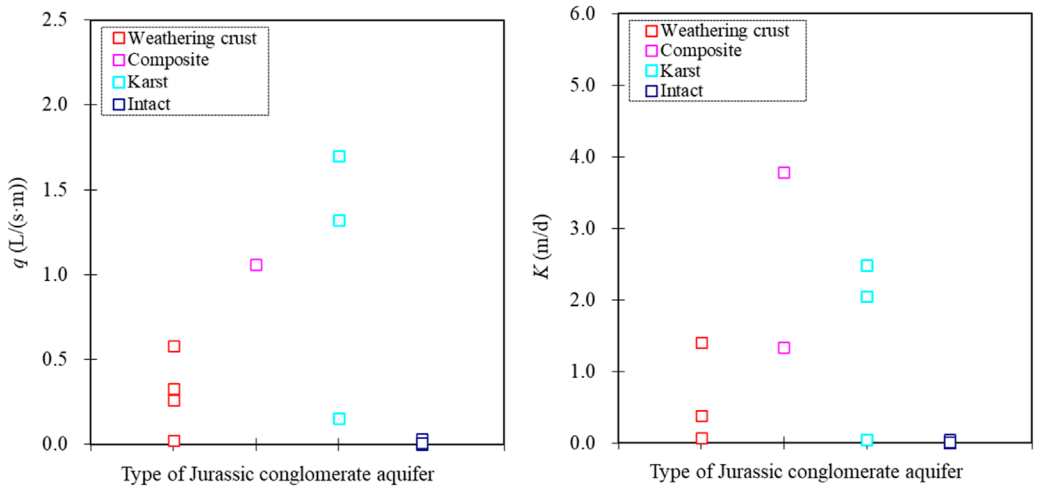

FIGURE 15
Comparison of hydrogeological parameters of different developmental types.

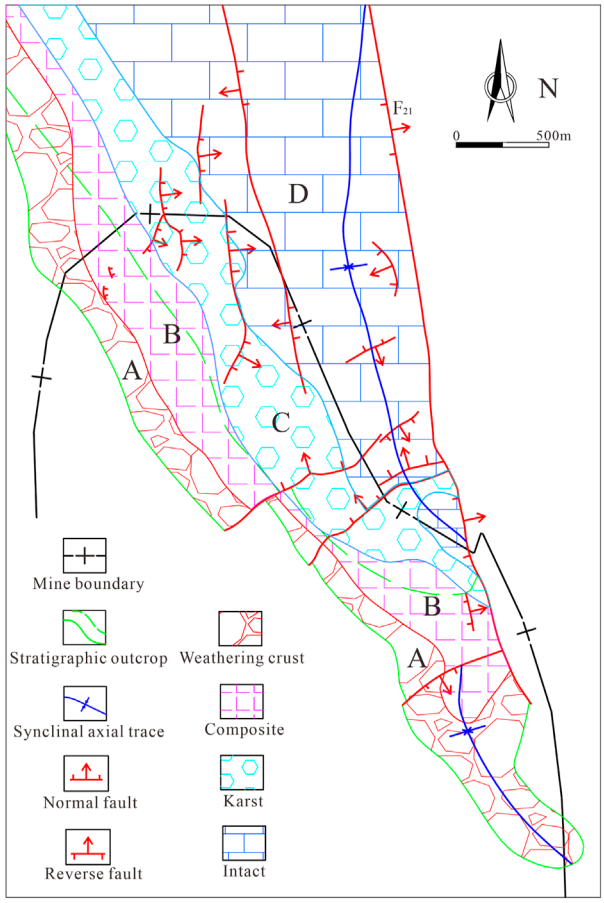

FIGURE 16
Plane zoning of Jurassic conglomerate aquifer structure.

the Jurassic conglomerate aquifer in the western and southern parts, showing a narrow NW-trending strip-shaped distribution. The top and bottom surfaces are angular unconformity interfaces, and the elevation is generally above - 250 m. The Jurassic conglomerate aquifer here has the characteristic of gradually thickening from west to east, but the overall thickness is relatively thin. The rock mass is severely weathered and broken, and karst is developed, showing the weathered crust type and composite type. However, affected by sediment filling, the water-bearing capacity is weak.

(2) Karst-composite zone (B): It is located near the concealed outcrop line of the top boundary of the Jurassic conglomerate aquifer in the western and southern parts, showing a narrow NW-trending strip-shaped distribution. The part above - 250 m elevation is of the weathered-crust type, and the lower part is of the karst type. The water-bearing capacity is strong.

(3) Runoff - karst zone (C): The thickness of the Jurassic conglomerate aquifer is relatively stable, and the burial depth increases from west to east. Karst is developed, and the vertical layered structure is relatively complex, showing the composite type and karst type. The water-bearing capacity is strong.

(4) Retention-intact zone (D): It is located at the turning end of the syncline in the eastern part, with a large burial depth. The bottom boundary elevation of the Jurassic conglomerate aquifer is generally below - 400 m. The rock mass is dense and intact, and karst does not develop, being of the intact type. The water-bearing capacity is weak.

In summary, the planar zoning of the Jurassic conglomerate aquifer generally shows a planar combination law of gradual transition from shallow to deep, from the limbs to the core of the syncline, and from the weathered-crust type to the composite type, karst type, and intact type.

5 Conclusion

(1) Vertically, the Jurassic system in Zhuxianzhuang coal mine can be divided into the upper sand-mudstone segment, the middle sand-gravel interbeds segment, and the lower conglomerate segment, showing the combined development characteristics of single-layer, double-layer, and triple-layer structures. The bottom conglomerate section exhibits significant heterogeneity due to the influence of later karstification and weathering. The morphology and extent of the Jurassic conglomerate aquifer are mainly affected by the morphology of the paleo-bedrock surface and late denudation, showing the characteristics of "thicker in the north and thinner in the south, thicker in the east and thinner in the west".

(2) Based on the logging responses of apparent resistivity (NR), artificial gamma (GG), caliper (CAL), and acoustic time-difference (AC), a rock mass structure identification model for the Jurassic conglomerate aquifer was established: type I (Intact section): High apparent resistivity (NR), low caliper (CAL), high artificial gamma (GG), low acoustic time-difference (AC); type III (Broken section): Low apparent resistivity (NR), high caliper (CAL), low artificial gamma (GG), high acoustic time-difference (AC); Type II (Relatively intact section): Logging parameters are between those of type I and type III. Model verification shows that when the degree of karst development and fragmentation increases, the proportion of type II + type III increases, and the RQD (Rock Quality Designation) decreases significantly.

(3) Based on the rock mass structure identification model, combined with the vertical distribution characteristics of the Jurassic conglomerate aquifer and the vertical differentiation of karst development, the Jurassic conglomerate aquifer was vertically divided into 4 development types: weathering crust type, karst type, composite type, and intact type.

(4) Combined with the classification of vertical structure types and the characteristics of planar distribution, the Jurassic conglomerate aquifer was divided into four types and six karst-developed zones. In the recharge-weathering zone (A), although the rock mass is broken and karst develops, the water-bearing capacity is affected by the restriction of sediment filling. Meanwhile, the retention-intact zone (D) exhibits weak water-earing capacity due to the intact rock mass and lack of karst development. The karst-composite zone (B) and the runoff-karst zone (C) are concentrated in the central NW-trending strip. Their karstification rates and hydrogeological parameters (q, K) are significantly higher than those in other regions, making them the main water-rich zones.

Data availability statement

The original contributions presented in the study are included in the article/supplementary material, further inquiries can be directed to the corresponding authors.

Author contributions

ZG: Conceptualization, Data curation, Formal Analysis, Investigation, Methodology, Software, Visualization, Writing – original draft, Writing – review and editing. JB: Methodology, Supervision, Writing – review and editing. LM: Investigation, Supervision, Writing – review and editing. SY: Investigation, Supervision, Writing – review and editing. CG: Investigation, Supervision, Writing – review and editing.

Funding

The author(s) declare that no financial support was received for the research and/or publication of this article.

Conflict of interest

The authors declare that the research was conducted in the absence of any commercial or financial relationships that could be construed as a potential conflict of interest.

Generative AI statement

The author(s) declare that no Generative AI was used in the creation of this manuscript.

Publisher's note

References

Barton, N., Lien, R., and Lunde, J. (1974). Engineering classification of rock masses for the design of tunnel support. *Rock Mech. Rock Eng.* 6 (4), 189–236. doi:10.1007/BF01239496

Cao, Z. B. (2020). Development mechanism of mining-induced water flowing fractures in different overburden structure of coal seam. dissertation. Beijing: China Coal Research Institute. doi:10.27222/d.cnki.gmkzy.2020.000015

Carrasquilla, A., and Lima, R. (2020). Basic and specialized geophysical well logs to characterize an offshore carbonate reservoir in the Campos Basin, southeast Brazil. *J. S. Am. Earth Sci.* 98, 102436. doi:10.1016/j.jsames.2019.102436

Chen, Y., Tang, D. Z., Xu, H., Lv, Y. M., and Chen, T. G. (2013). The distribution of coal structure in Hancheng based on well logging data. *J. China Coal Soc.* 08, 1435–1442. doi:10.13225/j.cnki.jccs.2013.08.002

Dlubac, K., Knight, R., Song, Y. Q., Bachman, N., Grau, B., Cannia, J., et al. (2013). Use of nmr logging to obtain estimates of hydraulic conductivity in the high plains aquifer, Nebraska, USA. *Water Res. Res.* 49 (4), 1871–1886. doi:10.1002/wrcr.20151

Fang, Z. W., and Zhang, L. Q. (2015). New approach to fine division and comparison of glutenite. *Fault-Block Oil Gas. Field.* 22 (03), 314–319. doi:10.6056/dkyqt201503010

Fu, X. H., Qin, Y., Wang, G. X., and Rudolph, V. (2009). Evaluation of coal structure and permeability with the aid of geophysical logging technology. *Fuel* 88, 2278–2285. doi:10.1016/j.fuel.2009.05.018

Gao, Y., and Li, Z. X. (2016). Logging interpretation of porosity for tight glutenite based on principal component analysis. *Acta Sedimentol. Sin.* 34 (04), 716–724. doi:10.14027/j.cnki.cjxb.2016.04.012

Guan, L. L., Gu, S. S., Wang, Z., and Cai, Y. Q. (2019). Geological evolution mechanism and comprehensive survey of K25 karst in Wudongde hydropower station. Adv. *Geophys.* 34 (01), 297–303. doi:10.6038/pg2019CC0002

Hatherly, P. (2013). Overview on the application of geophysics in coal mining. *Int. J. Coal Geol.* 114, 74–84. doi:10.1016/j.coal.2013.02.006

Hou, E. K., Che, X. Y., Long, T. W., Ye, Z. N., and Wen, Q. (2020). Prediction method of water inrush from ground cracks in shallow buried seams. *J. China Coal Soc.* 45 (12), 4154–4162. doi:10.13225/j.cnki.jccs.2020.0069

Hu, W. Y., and Tian, G. (2010). Mine water disaster type and prevention and control counter measures in China. *Coal Sci. Technol.* 38 (01), 92–96. doi:10.13199/j.cst.2010.01.97.huwy.026

Jiang, B., Qu, Z. H., Wang, G. G. X., and Li, M. (2010). Effects of structural deformation on formation of coalbed methane reservoirs in Huaibei coalfield, China. *Int. J. Coal Geol.* 82 (3), 175–183. doi:10.1016/j.coal.2009.12.011

Jiang, B., Qu, Z. H., Wang, J. L., Li, M., and Dou, X. Z. (2009). Research on coupling mechanism of mine structure and gas occurrence. *Procedia Earth Planet. Sci.* 1 (1), 1029–1036. doi:10.1016/j.proeps.2009.09.159

Karacan, C. O. (2009). Elastic and shear moduli of coal measure rocks derived from basic well logs using fractal statistics and radial basis functions. *Int. J. Rock Mech. Min.* 46 (8), 1281–1295. doi:10.1016/j.ijrmms.2009.04.002

Lai, Q., Xie, B., Wu, Y., Huang, K., Liu, X., Jin, Y., et al. (2017). Petrophysical characteristics and logging evaluation of asphaltene carbonate reservoirs: a case study of the Cambrian Longwangmiao Formation in Anyue gas field, Sichuan Basin, SW China. *Petrol. explor. Dev.* 44 (6), 941–947. doi:10.1016/S1876-3804(17)30106-4

Li, B., Wei, T., and Liu, Z. J. (2022). Construction of evaluation index system for water abundance of karst aquifers and risk assessment of water inrush on coal seam roof in Southwest China. *J. China Coal Soc.* 47 (S1), 152–159. doi:10.13225/j.cnki.jccs.2020.1407

Li, H., Qu, Z. H., Zhu, G. Y., Guo, L., Zhang, B. C., and Xue, Z. W. (2023). The structure formation mechanism and verification of "trending extrusion bending slip-trending translation" in Sudong syncline. *Geol. J. China Univ.* 29 (02), 261–271. doi:10.16108/j.issn1006-7493.2021042

Li, H. Y., Zhang, H. J., Li, S. C., Liu, R. T., Zheng, Z., and Bai, J. W. (2017). The seepage-flowing conversion mechanism of the fault lagging water inrush and its numerical simulation. *J. Min. Saf. Eng.* 34 (02), 323–329. doi:10.13545/j.cnki.jmse.2017.02.018

Lin, D. M., Shang, Y. J., Jin, W. J., and Ye, M. (2014). Preliminary Study of rock-physics and physical properties of rock mass structure. *J. Eng. Geol.* 22 (06), 1154–1158. doi:10.13544/j.cnki.jeg.2014.06.020

Liu, Z. D., Miao, F. Q., Hou, Q. Y., Luo, X. F., and Fu, D. (2013). Study on log response characteristics of Ordovician carbonate karst formation in area 5 of Tahe oilfield. *Adv. Geophys.* 28 (03), 1483–1489. doi:10.6038/pg20130343

Lopes, J. A. G., Medeiros, W. E., Oliveira, J. G., Santana, F. L., Araújo, R. E. B., Bruna, V. L., et al. (2023). Three-dimensional characterization of karstic dissolution zones, fracture networks, and lithostratigraphic interfaces using GPR cubes, core logs, and petrophysics: implications for thief zones development in carbonate reservoirs. *Mar. Pet. Geol.* 150, 106126. doi:10.1016/j.marpetgeo.2023.106126

Peng, S. P., Du, W. F., Yuan, C. F., Gou, J. W., and He, B. S. (2008). Identification and forecasting of different structural coals by P-wave and S-wave from well-logging. *Acta Geo* 10, 1311–1322. doi:10.3321/j.issn:0001-5717.2008.10.001

Ramadan, O., Idris, U., Steene, M. V., and Santoso, G. (2023). Combining nuclear magnetic resonance with deep and ultradeep azimuthal resistivity images in carbonate reservoirs links reservoir structure with rock type while drilling. *SPE* 000 (2-23MEOS), 7. doi:10.2118/213667-MS

Song, Z. Q., Hao, J., Tang, J. Q., and Shi, Y. K. (2013). Study on water inrush from fault's prevention and control theory. *J. China Coal Soc.* 38 (09), 1511–1515. doi:10.13225/j.cnki.jccs.2013.09.011

Tang, K. X., and Zhao, N. (2019). Geophysical characteristics and geological interpretation of karst strata. *Carsol. Sin.* 38 (04), 578–583. doi:10.11932/karst20190416

Teng, J., Yao, Y. B., Liu, D. M., and Cai, Y. D. (2015). Evaluation of coal texture distributions in the southern Qinshui basin, North China: Investigation by a multiple geophysical logging method. *Int. J. Coal Geol.* 140, 9–22. doi:10.1016/j.coal.2014.12.014

Wang, C. (2020). Breccia characteristics and reservoir identification in the eastern steep slope of Leijia area. *Pet. Geol. Eng.* 34 (04), 42–45+49. doi:10.3969/j.issn.1673-8217.2020.04.008

Wang, G. L., Jiang, B., Cao, D. Y., Zou, H., and Jin, W. J. (1998). On the Xuzhou-Suzhou arcuate duplex-imbricate fan thrust system. *Acta geo. Sin.* 72 (3), 228–236. doi:10.19762/j.cnki.dizhixuebao.1998.03.004

Wang, Y. Z. (2015). Evaluation of coal structure characteristics base on logging data. *China Coalbed Methane* 12 (04), 12–16. doi:10.3969/j.issn.1672-3074.2015.04.003

Wu, Z. H., Xu, S. Y., Liu, X. L., Wu, Y. H., Song, H. L., and Niu, L. J. (2016). Quantitative lithology identification technology of complex sand-conglomerate bodies. *Lithol. Reserv.* 28 (02), 114–118+126. doi:10.3969/j.issn.1673-8926.2016.02.016

Yin, S. L., Xue, X. J., Zhang, F., Hu, Z. X., Liu, Z. X., and Cheng, L. L. (2019). Productivity evaluation method of tight sandstone reservoir based on the logging curve. *J. Nat. Gas. Geosci.* 4 (3), 169–181. doi:10.1016/j.jnggs.2019.04.006

Zeng, Y. F., Zhu, H. C., Wu, Q., Wang, H., Guo, X. M., Cui, F. P., et al. (2024). Disaster-causing mechanism and prevention and control path of different types of coal seam roof water disasters in China. *J. China Coal Soc.* 49 (03), 1539–1555. doi:10.13225/j.cnki.jccs.2024.0039

Zhang, Y. J., and Zhang, Z. W. (2020). Research progress of mining overlying stratas failure law and control technology. *Coal Sci. Technol.* 48 (11), 85–97. doi:10.13199/j.cnki.cst.2020.11.011

Zhao, N., Wang, L., Tang, Y., Qu, J. H., Luo, X. P., and Sima, L. Q. (2016). Logging identification method for lithology: a case study of Baikouquan formation in Wellblock Fengnan, Junggar basin. Xinjiang Pet. *Geol.* 37 (06), 732–737. doi:10.7657/XJPG20160618

Zhu, G. Y., Jiang, B., and Zhu, S. G. (2018). Hydrogeological characteristics and prevention countermeasures of "fifth aquifer" in Zhuxianzhuang coal mine. *Coal Geol. Explor.* 46 (02), 111–117. doi:10.3969/j.issn.1001-1986.2018.02.017